ACS OMEGA

http://pubs.acs.org/journal/acsodf
Article

Initial Characterization of the Viridisins' Biological Properties

Ross Rayne Vermeulen,* Anton Du Preez van Staden, Tracey Ollewagen, Leonardo Joaquim van Zyl, Youran Luo, Wilfred A. van der Donk, Leon Milner Theodore Dicks, Carine Smith, and Marla Trindade

Cite This: *ACS Omega* 2024, 9, 31832−31841

ABSTRACT: Viridisin A1 and A2 were previously heterologously expressed, purified, and characterized as ribosomally produced and post-translationally modified lanthipeptides. Such lanthipeptide operons are surprisingly common in Gram-negative bacteria, although their expression seems to be predominantly cryptic under laboratory conditions. However, the bioactivity and biological role of most lanthipeptide operons originating from marine-associated *Pseudomonadota*, such as *Thalassomonas viridans* XOM25T, have not been described. Therefore, marine-associated Gram-negative lanthipeptide operons represent an untapped resource for novel structures, biochemistries, and bioactivities. Here, the upscaled production of viridisin A1 and A2 was performed for (methyl)lanthionine stereochemistry characterization, antibacterial, antifungal, and larval zebrafish behavioral screening. While antimicrobial activity was not observed, the VirBC modification machinery was found to install both DL- and LL-lanthionine stereoisomers. The VdsA1 and VdsA2 peptides induced sedative and stimulatory effects in zebrafish larvae, respectively, which is a bioactivity not previously reported from lanthipeptides. When combined, VdsA1 and VdsA2 counteracted the sedative and stimulatory effects observed when used individually.

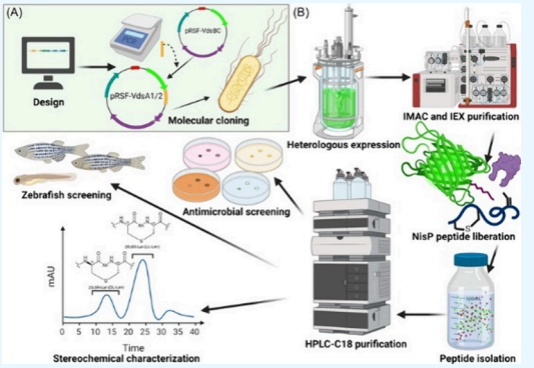

INTRODUCTION

Highly dissimilar ribosomally synthesized and post-translationally modified peptides (RiPPs) are immensely strong candidates for the discovery of useful molecules with potentially novel biochemistries and bioactivities. Unfortunately, most of these compounds remain undescribed due to two primary challenges: either the microbial producer fails to grow under laboratory conditions or the operons governing their production are tightly regulated and cryptic in a laboratory setting. Compared to classical top-down peptide discovery, bioinformatic mining allows for the identification of novel compounds, which are not always produced during top-down screening. Gram-negative marine bacteria are proving to be an interesting source of significantly dissimilar but cryptic RiPPs, harboring largely uncharacterized biochemistries and atypical bioactivities.[1−5]

Class I lanthipeptides use independent dehydratases and cyclases to post-translationally install lanthionine rings into the ribosomally synthesized precursor peptide, which consists of an N-terminal leader peptide and a C-terminal core peptide.[6] Class I dehydratases and cyclases are generally operon encoded and recognize the N-terminal leader for directed lanthionine ring synthesis. Briefly, Ser and Thr residues are dehydrated to form dehydroalanine (Dha) and dehydrobutyrine (Dhb), respectively.[7] The lanthionine thioether cross-linkages are installed by the operon-encoded cyclase through Michael-type addition of thiol side groups from Cys residues to the Dha or Dhb residues.[6] Cyclization of Cys thiols to Dha yields lanthionine (Lan), while cyclization with Dhb yields methyllanthionine (MeLan).[6]

The resulting (Me)Lan rings physically govern the three-dimensional structure and therefore bioactivities of these lanthipeptides.[8−11] However, Lan residues can assume two stereoisomer configurations, DL-Lan (2*S*,6*R*) or LL-Lan (2*R*,6*R*), while MeLan can form four possible stereoisomers.[12,13] To date, only the DL-MeLan (2*S*,3*S*,6*R*), LL-MeLan (2*R*,3*R*,6*R*), and D-*allo*-L-MeLan (2*S*,3*R*,6*R*) conformations have been observed while L-*allo*-L-MeLan (2*R*,3*S*,6*R*) remains elusive (Figure 1).[13]

Classic top-down screening has led to the discovery and characterization of valuable lanthipeptides with a broad range of bioactivities and robust tertiary structures.[14] For example, nisin is a widely used antimicrobial lanthipeptide used as a food preservative that may find therapeutic application in the future.[15−17] Some other biological functions of lanthipeptides include antivirals as seen in labyrinthopeptin A1 and divamides, morphogenic coordinators as seen with SapB in

Received: April 2, 2024
Revised: June 12, 2024
Accepted: June 18, 2024
Published: July 9, 2024

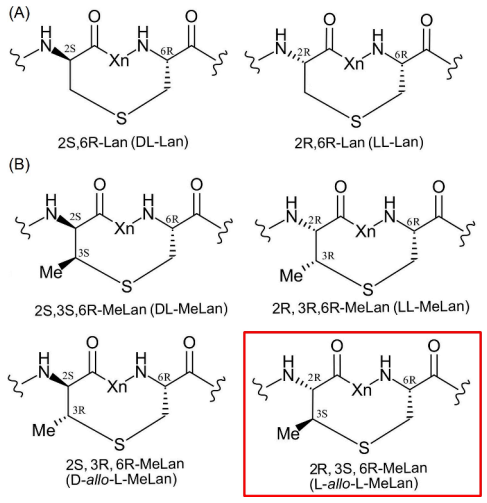

Figure 1. (A) Two possible stereoisomers can occur when Ser residues are dehydrated to Dha and conjugated to Cys thiol groups to form 2S,6R-Lan (DL-Lan) and 2R,6R-Lan (LL-Lan). (B) Four possible stereoisomers can occur when Thr is dehydrated to Dhb and conjugated to Cys thiols to form 2S,3S,6R-MeLan (DL-MeLan), 2R,3R,6R-MeLan (LL-MeLan), 2S,3R,6R-MeLan (D-*allo*-L-MeLan), and 2R,3S,6R-MeLan (L-*allo*-L-MeLan). The 2R,3S,6R-MeLan (L-*allo*-L-MeLan) stereoisomer highlighted by the red box has not yet been observed in nature.

filamentous *Streptomyces coelicolor*, and antifungals as seen in pinensin.[3,18−21] However, access to lanthipeptides via classic top-down screening is limited to bacterial producers, which grow and express their lanthipeptides under laboratory conditions. Heterologous expression of lanthipeptides has been a very useful tool during characterization or mechanistic studies as it generally offers a means to routinely access sufficient amounts of a given lanthipeptide.[14]

Although relatively high purities can be conveniently achieved using heterologous expression, drawbacks can include incorrect or incomplete post-translational modification and host toxicity resulting in low yields or unwanted adducts. Proper maturation is specifically challenging to engineer when attempting to characterize previously undescribed and significantly dissimilar lanthipeptides like those that are associated with unusual environmental Gram-negative bacteria and not Gram-positive bacteria from the gastrointestinal tract (GIT). The class I lanthipeptides, thalassomonasin A−B,[1] pseudorosin A−C,[5] ChmA,[22] RuiA,[22] PciA,[22] and PedA15.1/2,[23] originate from Gram-negative bacteria*Thalassomonas actiniarum* A5K-106,*Pseudoalteromonas flavipulchra* S16, *Chryseobacterium* sp. OV715,*Runella limosa* (WP_157607478), *Pseudoalteromonas citrea* DSM 8771, and*Pedobacter lusitanus* NL19, respectively, while the class II lanthipeptide, marinsedin, originates from the Gram-negative *Marinicella sediminis* F2T.[2] None of these environmental isolates are strongly associated with the GIT, but*T. actiniarum* A5K-106,[24]*P. flavipulchra* S16,[25] *Chryseobacterium* sp. OV715,[26]*P. citrea* DSM 8771,[27] and*Marinicella sediminis* F2T[28] are directly associated with the marine environment.

All seven of these lanthipeptide operons from Gram-negative bacteria were characterized via heterologous expression in *Escherichia coli*, as these operons are cryptic under laboratory conditions. Although marinsedin displays cytotoxic activity against select cancer lines,[2] these Gram-negative lanthipeptides did not show the antimicrobial activity patterns observed in many lanthipeptides from Gram-positive bacteria. Therefore, the precise biological role(s) of lanthipeptides derived from Gram-negative marine bacteria remains largely enigmatic and is complicated by their cryptic nature, which currently limits their production to heterologous expression.

The viridisin lanthipeptides, VdsA1 and VdsA2, have only been accessed through heterologous expression systems in *E. coli*.[29] The VdsA1 peptide, $[M-4H2O + nH]^{n+}$ (n = 2, 3, 4), has one MeLan and three Lan rings while the VdsA2 peptide $[M-5H2O + nH]^{n+}$ (n = 2, 3) has two Lan rings.[29] During HPLC-PR purification, VdsA1 and VdsA2 each produced two species (Figure 2). The two VdsA1 species, P1A and P1B, have

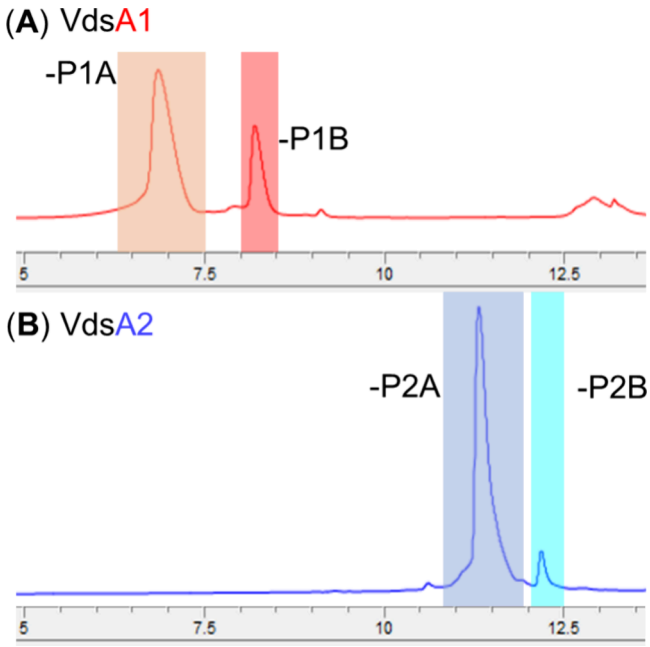

Figure 2. (A) HPLC-C_8 separation of the VdsA1 isomers -P1A (M_r: 2732.297) and -P1B (M_r: 2732.294), which have identical monoisotopic masses and fragmentation spectra. (B) HPLC-C_8 separation of the VdsA2 species where -P2A (M_r: 2993.189) is bound to a GSH modification and -P2B (M_r: 2686.106) is not. The fragmentation spectra of P2A and P2B species indicate that they share a regiospecific lanthionine ring formation pattern.

identical monoisotopic masses, while the majority of VdsA2 was bound to a glutathione adduct (Figure 2). In this work, larger quantities of the VdsA1 and VdsA2 peptides at high purities were used to characterize the (Me)Lan stereoisomer composition of the viridisin A1 isomers (VdsA1-P1A and VdsA1-P1B). Then, the viridisin VdsA1-P1A stereoisomer and VdsA2 species' antimicrobial and antifungal activities were screened. Finally, a zebrafish light−dark transition assay was used to determine if the VdsA1-P1A and VdsA2-P2A species had any effect on behavioral responsiveness.

RESULTS AND DISCUSSION

The biological roles and activities of most lanthipeptides from Gram-negative bacteria have yet to be elucidated. This is an especially challenging task for the heterologously expressed thalassomonasin A−B,[1] pseudorosin A−C,[5] ChmA,[22] RuiA,[22] PciA,[22] PedA15.1/2,[23] and viridisin[29] lanthipeptides. Due to their cryptic nature, the leader peptide cleavage sites, dehydration states, and ring topologies for thalassomonasin A−B,[1] pseudorosin A−C,[5] ChmA,[22] RuiA,[22] PciA,[22]

https://doi.org/10.1021/acsomega.4c03149
ACS Omega 2024, 9, 31832−31841

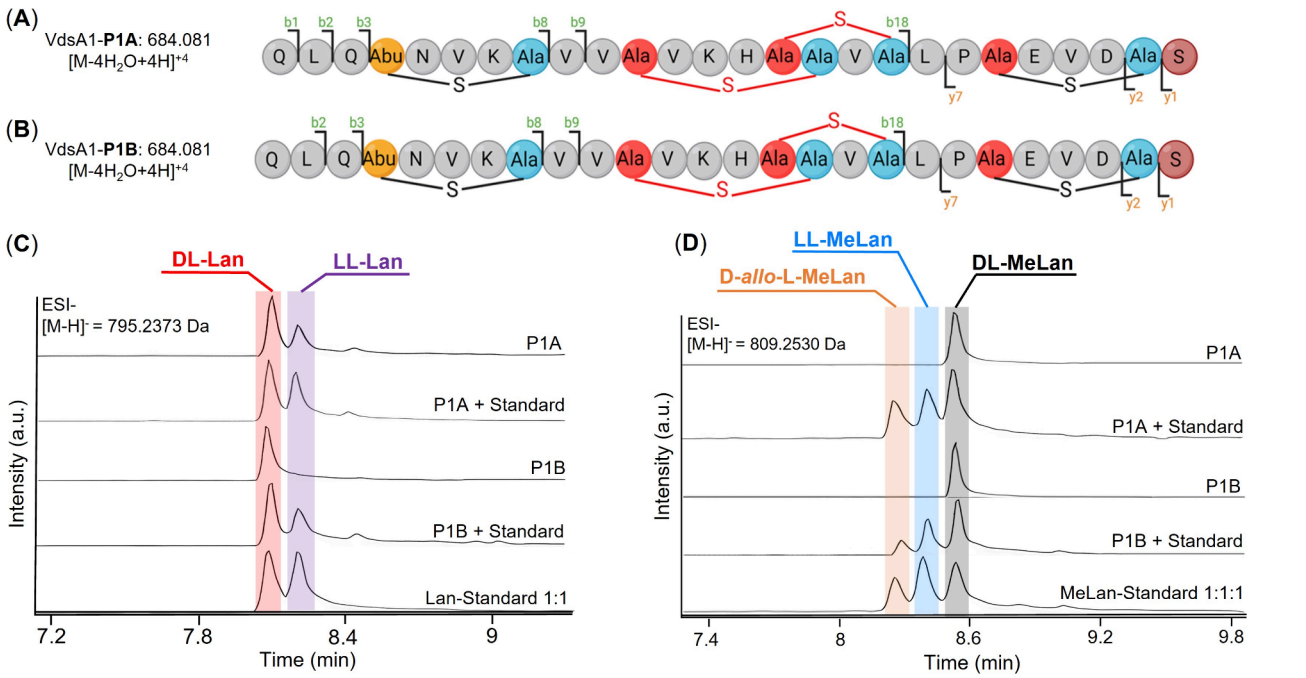

Figure 3. (A) VdsA1-P1A parent ion m/z and fragmentation pattern while (B) VdsA1-P1B species elutes later than VdsA1-P1A, as seen in Figure 2A, but shows an identical parent ion m/z and fragmentation pattern. (C) Lanthionine stereoisomer composition of (A) VdsA1-P1A and (B) VdsA1-P1B, indicating that (A) VdsA1-P1A contains both DL- and LL-Lan residues. (D) Methyllanthionine stereoisomer composition of (A) VdsA1-P1A and (B) VdsA1-P1B indicating that both species only contain the DL-MeLan residue.

PedA15.1/2,[23] and viridisin[29] remains unconfirmed. Incomplete modification or incorrect maturation due to improper heterologous expression can significantly impact their bioactivities, or lack thereof. These unconfirmed structures have created a gridlock during bioactivity testing; without verification, it is impossible to definitively prove whether these peptides lack specific bioactivities. However, at this stage in our understanding of lanthipeptides from Gram-negative bacteria, it is equally possible that these peptides fulfill biological roles outside of antibacterials, by potentially inducing novel bioactivities.

Previously, the *vds* class I lanthipeptide operon from *Thalassomonas viridans* XOM25T was used to construct an*E. coli*-based expression system to produce modified VdsA1 and VdsA2 peptides.[29] Heterologous expression, purification, and mass spectral analysis of the VdsA1 and VdsA2 peptides indicated that two forms of each peptide could be detected (Figure 2). The VdsA1 peptide splits into the VdsA1-P1A and VdsA1-P1B species, which have identical monoisotopic masses and fragmentation patterns but different retention times during HPLC-C_{18} purification (Figure 2A).[29] On the other hand, VdsA2 peptide splits into one dominant species, -P2A, which was bound to a glutathione (GSH) modification via thioether cross-linking with a Dhb residue. The other species from VdsA2, VdsA2-P2B, was not bound to GSH but carried an identical dehydration state and ring topology to VdsA2-P2A (Figure 2B).[29]

Upscaled Production of VdsA1 and VdsA2 Peptides. Approximately 220 mg of the GFP-VdsA1 and 200 mg of GFP-VdsA2 fusion proteins were purified from 14 L of the*E. coli* pRSF-VdsA1 and -VdsA2 cultures (coexpressing Vds-B and -C) using IMAC and IEC, respectively.[29] The GFP-VdsA1 and -VdsA2 fusion proteins were cleaved at a 1:1 v/v ratio of NisP-mCherry (Supporting Information) to GFP-VdsA1/A2. Peptide liberation from GFP-fusion partners was confirmed using fluorescent imaging semi-native SDS-PAGE analysis (Figure S2). After NisP-mCherry cleavage, the VdsA1 and VdsA2 peptides were isolated by 75% v/v acetonitrile precipitation of the GFP-fusion partner and NisP-mCherry protease.

Analytical HPLC-C_8 and subsequent HPLC-C_{18} purification of VdsA1 produced 7.05 mg of the VdsA1-P1A isomer and 2.36 mg of the VdsA1-P1B isomer at 92 and 95% purities, respectively (Figures S3 and S4). Analytical HPLC-C_8 and -C_{18} purification of VdsA2 produced 5.77 mg of VdsA2-P2A bound to GSH and 0.94 mg of VdsA2-P2B without GSH at 93 and 79% purity, respectively (Figures S5 and S6). Purities were determined by HPLC-C_{18} analysis (Figures S4−S6).

Stereochemical Analysis of VdsA1-P1A and -P1B Stereoisomers. In line with the search for new lanthipeptide structures from atypical modification machinery, the stereochemistry of the VdsA1-P1A and VdsA1-P1B isomers was characterized. The VirCB modification machinery installed both DL- and LL-Lan stereoisomers but only installed the DL-MeLan stereoisomer in the VdsA1-P1A and -P2A (Figure 3). This mixture of DL- and LL-Lan residues has been previously observed for the lanthipeptide PedA15.1 and can also explain the observed differences in the VdsA1-P1A and -P1B hydrophobicity (Figure 2).[23] The PedA15.1 and viridisin dehydratase and cyclase machinery is more closely related when compared to other class I lanthipeptides from Gram-positive bacteria.[29] However, PedA15.1 does not contain any MeLan residues, which makes it difficult to compare with VdsA1, although upon Ser to Thr substitution, the PedA15.1/2 machinery was able to install both the DL- and LL-MeLan configurations.

While the L-*allo*-L-Melan residue remains elusive, even to the significantly dissimilar modification machinery like those for viridisin and PedA15.1, recent findings might unlock its biosynthetic pathway along with other stereoisomers. The

https://doi.org/10.1021/acsomega.4c03149
ACS Omega 2024, 9, 31832−31841

Table 1. Antimicrobial Activity Screen at 10 μM

microorganism	VdsA1(P1A) and VdsA2(+GHS)	VdsA1(P1A) and VdsA2	VdsA1(P1A)	VdsA2(+GHS)
Bacteria				
Staphylococcus aureus subsp. *aureus* ATCC 25923	-	-	-	-
Staphylococcus aureus subsp. *aureus* strain E2125	-	-	-	-
Pseudomonas aeruginosa PAO1	-	-	-	-
Pseudomonas aeruginosa ATCC 27853	-	-	-	-
Klebsiella pneumoniae K6 (ATCC 700603)	-	-	-	-
Enterobacter cloacae ATCC 13047	-	-	-	-
Escherichia coli ATCC 25299	-	-	-	-
Bacillus subtilis ATCC 21332	-	-	-	-
Vibrio harveyi LMG 4044	-	-	-	-
Vibrio ruber LMG 23124	-	-	-	-
Thalassomonas viridans XOM25T	-	-	-	-
Yeast				
Saccharomyces cerevisiae S288C	-	-	-	-
Cryptococcus neoformans H99	-	-	-	-
Candida albicans CAB 1084	-	-	-	-

dethiolation activity observed in the pseudorosin dehydratase may offer an alternative mechanism of thioether-cross-linkage formation.[5] Rethiolation of Dha residues, derived from cysteine, during an alternative or backdoor lanthionine ring formation mechanism, may allow for the formation of exotic (Me)Lan stereochemistries.

The VdsA2 peptide also splits into two species during HPLC reverse phase purification, which were denoted VdsA2-P2A and VdsA2-P2B; however, the GSH modification was identified in the P2A spectra (Figure 2). The GSH modification disqualified VdsA2-P2A from lanthionine stereochemical analysis, and the VdsA2-P2B species could not be analyzed due to insufficient quantities, which is commonly reported for heterologously expressed lanthipeptides from Gram-negative bacteria.[1,5,21] The addition of GSH modification is commonly observed in many other heterologously expressed class-I lanthipeptides from Gram-negative bacteria. The ChmA and RuiA lanthipeptides contained multiple GSH modifications at various intermediate dehydration states.[22]

Coexpression of the native producer's glutamyl-tRNA synthetase and $tRNA^{Glu}$ lowered the amount of partially dehydrated species; however, ChmA and RuiA were still glutathionylated.[22] As seen with the thalassomonasins, heterologous expression of viridisins did not require coexpression of the glutamyl-tRNA synthetase, and $tRNA^{Glu}$ from *T. viridans* as the fully modified species was the most abundant ion.[1,29] Successful dehydration is likely because *E. coli* and *T. viridans* both belong to the Gammaproteobacteria class while *Chryseobacterium* sp. OV715 and *Runella limosa* differ from *E. coli* at the phylum level. In addition, the VdsA1 and VdsA2 peptides were expressed as GFP-fusion constructs, which might have aided compatibility between VirB and the foreign glutamyl-tRNA synthetase and $tRNA^{Glu}$. Finally, the GSH modification has also been detected in pseudorosins (PsfA1−3) identified in *P. flavipulchra* S16 and the class II lanthipeptide marinsedin from *Marinicella sediminis* $F2^T$.

Antimicrobial and Antifungal Screening of VdsA1 and VdsA2. The VdsA1-P1A, VdsA2-P2A, and VdsA2-P2B were tested individually and in combination at a 10 μM concentration. No antimicrobial activity was observed in these treatments against the select ESKAPE pathogens, *Vibrio* spp., or yeast (Table 1).

Zebrafish Light−Dark Transition Test. Although the most reported bioactivity for lanthipeptides is antibacterial, lanthipeptides exhibit a wide range of bioactivities. Marinsedin[2] and pinensin[21] are the only two lanthipeptides from Gram-negative bacteria which were isolated from the native producer. Marinsedin,[2] a class II lanthipeptide, shows cytotoxicity, while the class I lanthipeptide pinensin[21] shows antifungal activity. This might suggest that the dissimilar lanthipeptides from marine-associated Gram-negative bacteria in general may have biological functions beyond antibacterial activity. However, committing exceptionally dissimilar compounds, like lanthipeptides, from Gram-negative bacteria to broad and exhaustive target-based discovery platforms can quickly become unfeasible.

The thalassomonasins, pseudorosin A−C, and PedA15.1/2,[23] and now the viridisin peptides, have been screened against a range of microorganisms; however, antimicrobial activity has not been detected. While it is possible that these lanthipeptides are not correctly produced by the heterologous producer *E. coli*, it is also possible that they have other, potentially novel bioactivities beyond antimicrobial properties. To address the lack of antimicrobial activity seen in the viridisins, the more abundant VdsA1-P1A isomer and both VdsA2 species, with and without GSH, were used for phenotypic screening using the zebrafish model.

Although target-based discovery is considered the more modern approach to the highly complex task of drug discovery,[30] phenotypic-based discoveries are regaining popularity.[31,32] While target-based discovery follows a more rational approach where a given target is decided upon beforehand, phenotypic approaches can elucidate the therapeutic relevance on a broad spectrum of known and yet-to-be-defined targets.[31,33] The zebrafish model is a powerful phenotypic screening platform capable of elucidating activities on yet-to-be-determined targets in drug discovery without the need for a defined molecular mechanism. This is due to the model's ability to transcend the limitations of *in vitro* models and relay systemic information relating to pain, sedation, and gut mobility, which are all disease-relevant phenotypes.[34,35] The zebrafish model allows for live testing on whole, higher organisms that harbor defined organs like a nervous system, liver, heart, and kidneys, which perform similar functions in humans.[34,35] Zebrafish screening has massive application

https://doi.org/10.1021/acsomega.4c03149
ACS Omega 2024, 9, 31832−31841

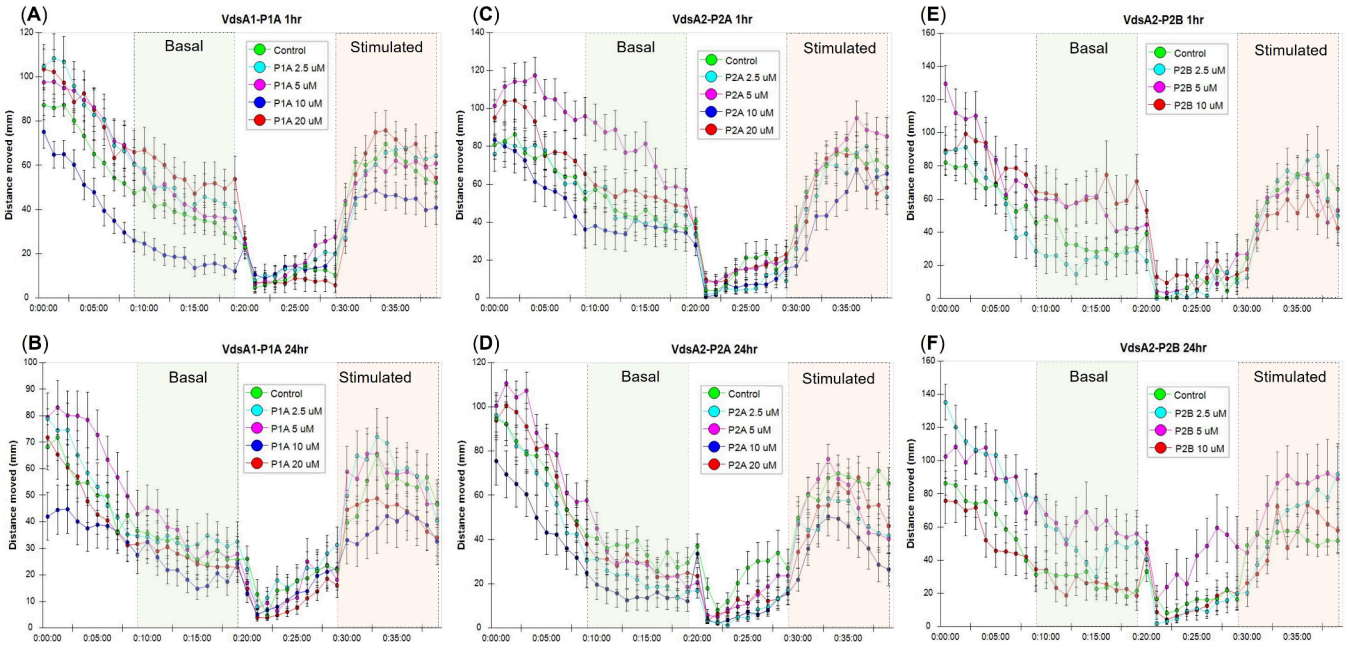

Figure 4. The VdsA1-P1A, VdsA2-P2A, and VdsA2-P2B peptides' effect on zebrafish larvae (<5 dpf) behavior at various concentrations. (A) VdsA1-P1A effect after 1 h and (B) after 24 h. (C) VdsA2-P2A effect after 1 h and (D) after 24 h. (E) VdsA2-P2B effect after 1 h and (F) after 24 h. The 10−20 min range (green boxes) and 30−40 min time range (orange boxes) were considered the base level and excited zebrafish behavioral states, respectively. The total distance at which each group moved over these time periods was used for statistical comparison within treatment, results of which are summarized in Table 1. Locomotive data is presented as 1 min bins, where each point represents the means with SEM ($n \geq 16 \leq 40$).

Table 2. Statistically Significant Effects on Zebrafish Behavior

	basal 10−20[a] (1 h)	stimulated 30−40[b] (1 h)	basal 10−20 (24 h)	stimulated 30−40 (24 h)
VdsA1-**P1A**	↓10 μM: $p = 0.028$[c,e]	no effect	no effect	no effect
VdsA2-**P2A**	↑5 μM: $p = 0.020$[d]	no effect	↓10 μM: $p = 0.020$	no effect
VdsA2-**P2B**	no effect	no effect	no effect on means[e]	no effect on means[e]

[a]10−20 indicates the time frame used to quantify the preillumination (base level) effect. [b]30−40 indicates the time frame used to quantify the postillumination (stimulated state) effect. [c]↓ represents a sedative effect. [d]↑ represents a stimulatory effect. [e]Heterogeneous variance in the group.

potential in the characterization of RiPPs such as lanthipeptides, especially for producer organisms that live symbiotically in a holobiont environment where interspecies communication and collaboration are fundamental.

The zebrafish light−dark transition test (LDTT), which produces a highly reproducible, robust response to bright light exposure—allowing for demonstration of basal activity levels, as well as anxiety-like hyperlocomotion behavior—is particularly useful in screening for the potential psychoactivity of a novel compound while simultaneously monitoring toxicity risk. The effects of the VdsA1-P1A, VdsA2-P2A, and VdsA2-P2B lanthipeptides were initially tested individually. VdsA1-P1A and VdsA2-P2A were administered at 2.5, 5.0, 10.0, and 20.0 μM while VdsA2-P2B was only tested at 2.5, 5.0, and 10.0 μM due to limited supply. For the same reason, the number of replicates in each treatment (n) was lowered from 24 for VdsA1-P1A and VdsA2-P2A to 16 for VdsA2-P2B (full statistical analysis Figures S7−S18).

Figure 4A−F represents the activity tracks through the LDTT assay for the VdsA1-P1A, VdsA2-P2A, and VdsA2-P2B lanthipeptide treatments after exposure for 1 h (Figure 4A,C,E) and 24 h (Figure 4B,D,F), respectively. The level of larval locomotion was quantified by allowing a 10 min acclimation period whereafter the larval basal activity was quantified for a further 10 min period (Figure 4, green shaded area over 10−20 min). The larvae were then illuminated with bright white light for 10 min to induce an anxiety-like response. Upon returning to dark conditions, the larval stimulated state was quantified over 10 min (Figure 4, orange shaded area over 30−40 min). Table 2 summarizes the dosages that caused a significant change in zebrafish larvae' total locomotion over the basal and stimulated periods for 1 and 24 h exposure seen in the figure. The VdsA1-P1A lanthipeptide had a statistically significant sedative-like effect at 10 μM after 1 h of exposure in the basal state when compared to the control (Table 2 and Figure 4A, blue curve vs green control curve during the basal period). This sedative effect at 10 μM likely disturbed the homogeneity of larval basal locomotion variances, as a p-value <0.001 was obtained for Levene's test (Figure S7). The observed effect of Vds A1-P1A was not maintained after continued exposure at 28 °C. The VdsA1-P1A peptide elicited a sedative effect that resembles the profile demonstrated for the potent sedative diazepam, albeit somewhat milder. This observation, together with the transient nature of the effect, argues against toxicity and suggests that a neurological effect might be at play.

In contrast, the VdsA2-P2A peptide that contains the GHS modification caused a stimulatory effect at 5 μM only during the basal state after 1 h exposure (Table 2, Figure 4C pink curve vs green control curve during the basal period, and

https://doi.org/10.1021/acsomega.4c03149
ACS Omega 2024, 9, 31832−31841

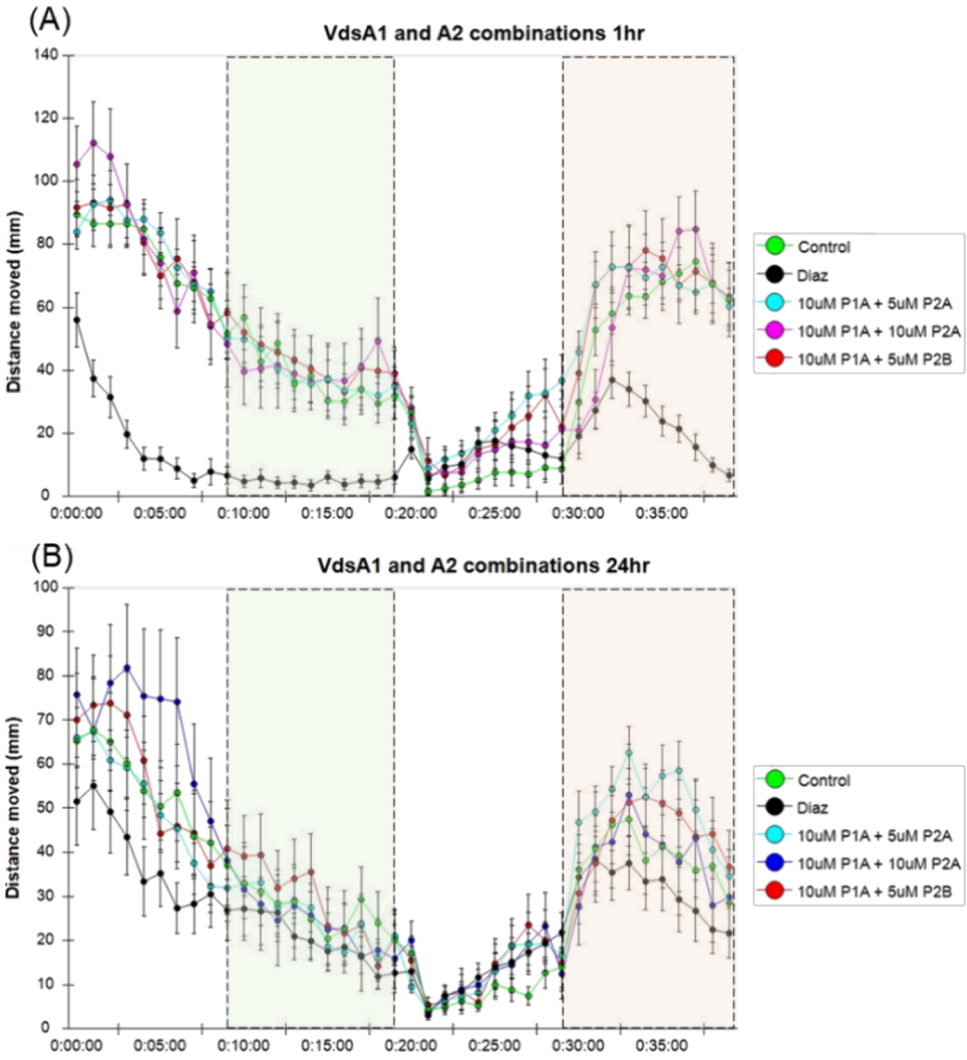

Figure 5. The effective dosages of VdsA1-P1A, VdsA2-P2A, and VdsA2-P2B were combined for retreatment investigating potential synergistic effects after (A) 1 and (B) 24 h. The 10−20 min range (green boxes) and 30−40 min time range (orange boxes) were considered the basal and excited zebrafish behavioral states, respectively. The total distance at which each group moved over these time periods was used for statistical comparison within treatment. No statistically significant changes in zebrafish behavior were observed at known effective dosages during the base level and excited states. Therefore, the previous sedative and stimulatory effects seen for VdsA1-P1A and VdsA2-P2A and -P2B were counteracted upon cotreatment. Locomotive data is presented as 1 min bins, where each point represents the means with SEM ($n \geq 16 \leq 40$).

Figure S11). After 24 h, a sedative or relatively hypolocomotive state was then observed at 10 μM VdsA2-P2A during the basal period (Table 2 and Figure 4D blue curve vs green curve). However, this data appears to be non-normally distributed where the one-way ANOVA p-value was 0.145 but the Kruskal−Wallis p-value was 0.002 and Fisher's LSD post hoc p-value = 0.02 for the 10 μM vs the control.

The reduced thiol from cysteine in GSH is key to its antioxidant activities and ability to neutralize harmful reactive oxygen species in biological systems. However, this thiol is covalently bound to VdsA2-P2A through a thioether linkage, which is not reversible like the disulfide bonds that normally form between GSH molecules. Therefore, it is difficult to predict the behavior and effect of the glutathione adduct on the zebrafish larvae. It must still be determined if GSH is an unwanted adduct originating from heterologous expression in *E. coli* or if GSH binding is a characteristic of lanthipeptides from marine-associated Gram-negatives. In this work, the majority of the VdsA2 lanthipeptide is bound to GSH. While GSH modifications are not commonly reported in natively produced lanthipeptides from Gram-positive bacteria, future work should consider the fact that the GSH biosynthetic pathway and biological role are probably more similar between *E. coli* and other Gram-negative lanthipeptide producers. Alignment of the*E. coli* glutamate-cysteine ligase (GshA) with the*T. viridans*-translated genome using the BLAST function[36] indicates a protein match with an *E*-value = $1e^{-142}$ (88% coverage, 49% identities, 67% positives, and 0% gaps). In lactic acid bacteria, which commonly produce lanthipeptides, GSH is reported at significantly lower concentrations compared to*E. coli*.[37,38]

The VdsA2-P2B peptide has the same ring structure and dehydration state as VdsA2-P2A; however, it is not bound to the GSH modification. Similar to the VdsA2-P2A peptide, the VdsA2-P2B peptide induced a statistically near-significant, one-way ANOVA p = 0.061 and Levene's test p = 0.012 (Figure S15B) stimulatory effect on larval locomotion during the basal state after 1 h exposure (Table 2; Figures S15−S18). Heterogeneity in group variance was observed after 24 h exposure to VdsA2-P2B during the basal and stimulated states

https://doi.org/10.1021/acsomega.4c03149
ACS Omega 2024, 9, 31832−31841

(Figures S17B and S18B, with Levene's test p-values <0.001). In addition, VdsA2-P2B seemed to maintain its near-significant stimulatory effect on basal locomotion after 24 h (Welch test, $p = 0.053$), most significantly at the 5 μM dosage (Figure 4F, purple curve vs green control curve and Figure S17; Games-Howell *post hoc*, $p = 0.077$).

The effect of various VdsA1-P1A, VdsA2-P2A, and VdsA2-P2B treatments in combination was then assessed. In combination, the sedative and stimulatory effects observed for the individual peptide treatments were abolished (Figure 5 and Figures S19−S22). The decrease in bioactivities upon cotreatment suggests a potential counteractive relationship among the VdsA1-P1A, VdsA2-P2A, and VdsA2-P2B peptides. Diazepam was added as a positive treatment control to reflect the typical response expected after exposure to a sedative. Diazepam's effect is evident acutely after 1 h of exposure but not maintained after 24 h (Figure 5, black curve).[39]

Finally, the effect of trifluoroacetic acid (TFA) on zebrafish larvae was measured from 3.125 to 200 μM to ensure any residual TFA from HPLC purification had no effect on larval behavior. No changes in behavior were observed after 1 and 24 h exposure in both the basal or stimulated states for any concentration, nor was the homogeneity of group variances disturbed (Figures S23−S26).

Following exposure to various doses of all peptides and relevant concentrations of vehicle TFA, all zebrafish larvae were observed microscopically for signs of toxicity, such as body axis deviations, cardiac and yolk sac edema, or loss of pigmentation. No signs of toxicity were observed.

EXPERIMENTAL METHODS

General Materials and Reagents. All growth media components and reagents were sourced from Merck (Darmstadt, Germany) unless stated otherwise.

Molecular Techniques. Cloning was performed according to standard protocols described by Sambrook et al. and Ausubel.[40,41] Plasmid DNA extractions were performed using the PureYield Plasmid Miniprep System (Promega, United Kingdom) according to the manufacturer's instructions. Restriction enzymes (REs) and T4 DNA ligase were used according to the manufacturer's instructions (New England Biolabs). Amplification of DNA via polymerase chain reaction (PCR) was performed using Q5 DNA polymerase (NEB).

Oligonucleotides were designed using the CLC main workbench program (CLC bio, Aarhus, Denmark) and purchased from Inqaba Biotechnical Industries (Pretoria, South Africa). DNA sequencing was performed by the Central Analytical Facilities (CAF) at the University of Stellenbosch, South Africa.

Agarose gel electrophoresis was used for the analysis and purification of RE-digested DNA fragments in TBE buffer at 10 V/cm using an Ephortec 3000 V power supply (Triad Scientific, Manasquan, New Jersey, USA). Excised gel DNA fragments were purified using the Zymo Gel Extraction Kit (D4001, Zymo Corporation, USA).

Upscaled Production and Purification of VdsA1 and VdsA2. Heterologous expression of the GFP-VdsA1 and -VdsA2 fusion proteins was performed in 3.5 L batches using the Minifor 5 L fermenter (Minifors, Infors AG, CH-4103 Bottmingen/Basel, Switzerland) up to a final volume of 14 L, respectively. Briefly, 3.15 L of terrific broth with 0.01% antifoam 204 (Sigma-Aldrich) was autoclaved in the 5 L Minifors bioreactor. After cooling, 350 mL of sterilized 10× TB buffer and kanamycin (50 μg/mL final concentration) was aseptically added. Overnight cultures (35 mL in LB broth 50 μg/mL kanamycin) of the*E. coli* Bl21(DE3) pRSF-VdsA2 and pRSF-VdsA2 were respectively used to inoculate each 3.5 L batch and grown at 36 °C with agitation (150 rpm) and aeration (1 L of sterile compressed air per minute). At an optical density of 0.6 (OD 590 nm), the temperature was lowered to 21 °C and 0.15 mM IPTG was used to induce the expression of either GFP-VdsA1 or GFP-VdsA2, respectively.

After 48 h at 21 °C, each batch was harvested and centrifuged at 10,000 *g* for 7 min and resuspended in 15 mL SB per gram of wet cell mass. Cells were resuspended with orbital shaking for 15 min at 4 °C and then frozen at −20 °C. Cell lysis was performed with the addition of 1 mg/mL lysozyme, incubation on ice for 30 min, and sonication for 10 min (5 s pulse, 5 s pause) at 50% amplitude. RNaseI and DNaseI were added to a final concentration of 10 and 5 μg/mL respectively.

The lysate was cleared by centrifugation at 18,000 *g* for 35 min and loaded onto 30 mL of NINTA His•Bind resin (Sigma 69670-M). The loaded resin was washed with 10 CVs SB20 (50 mM Tris, 500 mM NaCl, 20 mM imidazole, pH 8.3) and eluted in SB500 (50 mM Tris, 500 mM NaCl, 500 mM imidazole, pH 8.3). The eluent in SB500 was diluted 35 times with AB (50 mM Tris, pH 8.3) and loaded onto a 25 mL DEAE−Sepharose column (Sigma DFF100). The loaded resin was washed with 10 CV of AB50 (50 mM Tris, 50 mM NaCl, pH 8.3) and eluted in AB150 (50 mM Tris, 150 mM NaCl, pH 8.3). Thereafter, the column was washed with AB1000 (50 mM Tris, 1000 mM NacL, pH 8.3) and re-equilibrated in AB buffer. The GFP-VdsA1 and GFP-VdsA2 AB150 eluents were sterilized using a 0.2 μM CA syringe filter (GVS, FJ25ASCCA004FL01) and stored at −20 °C until cleavage using NisP-mCherry.

Similarly, NisP-mCherry was heterologously expressed in 3.5 L batches using the same method until a total volume of 10.5 L was achieved and then harvested and lysed as described as above. Cleared lysate containing the NisP-mCherry fusion protein was purified as described; however, once the DEAE Sepharose resin was loaded with NisP-mCherry, it was washed with AB20 (50 mM Tris, 20 mM NaCl, pH 8.3) and eluted with AB150. NisP-mCherry was filter sterilized and added to an equal volume of GFP-VdsA1 or GFP-VdsA2, respectively. The cleavage mixture was incubated for 12 h at 26 °C in a sterile glass Schott bottle containing five times the total cleavage volume.

After cleavage, the mixture was frozen at −80 °C and lyophilized using a freeze-dryer (VirTis BenchTop K Series, USA). After lyophilization, three times the cleavage volume of 75% acetonitrile was used to isolate VdsA1 and 65% acetonitrile was used to isolate VdsA2 from respective mixtures. The respective acetonitrile resuspensions were placed on an orbital shaker (50 rpm) at 26 °C for 30 min. The majority of cleaved GFP and NisP-mCherry precipitated. The acetonitrile solution containing the respective VdsA1 or VdsA2 peptides was then centrifuged at 5000 *g* for 10 min at 21 °C.

The VdsA1 isomers, P1A and P1B, were separated using HPLC (Agilent 1260 Infinity LC System, Agilent Technologies, UK) reverse phase chromatography and purified using the C_8 (Zorbax 300SB-C_8 RP, Agilent Technologies) and C_{18} (Zorbax 300SB-C_{18} RP, Agilent Technologies) columns after lyophilization. Likewise, the VdsA2 species, with and without GHS, was separated using HPLC-C_8 reverse phase chromatography followed by C_{18} purification.

https://doi.org/10.1021/acsomega.4c03149
ACS Omega 2024, 9, 31832−31841

After HPLC-C_{18} purification, the samples were lyophilized, analytically weighted off using the XP26 Excellence Plus Micro Balance (Mettler Toledo, Columbus, Ohio, USA), and resuspended in sterile ultrapure water. The purity of the samples was determined by injecting 90 μL of 20 μM sample and analyzed with HPLC-C_{18} using a linear gradient of 0−100% B (A: analytical quality water +0.1%TFA, B: acetonitrile +0.1% TFA) over 35 min.

Stereochemical Analysis of VdsA1-P1A and -P1B Stereoisomers. Stereochemical analysis of the VdsA1-P1A and VdsA1-P1B isomers was performed according to a recently described method.[42] Briefly, 0.05 mg samples of VdsA1-P1A and VdsA1-P1B were hydrolyzed under acidic conditions and derivatized with 1-fluoro-2,4-dinitrophenyl-5-L-leucine amide as described. Subsequently, these samples were analyzed by LC-MS using an Agilent 6545 LC/Q-TOF instrument equipped with a Kinetex F5 Core−Shell HPLC column (1.7 μm F5 100 Å, LC Column 100 × 2.1 mm). The stereochemistry of Lan and MeLan diastereomers was determined through comparison and coinjection with Lan and MeLan standard samples, which included DL-Lan, LL-Lan, DL-MeLan, LL-MeLan, and D-*allo*-L-MeLan diastereomers.

Antimicrobial and Antifungal Activity Screening of VdsA1 and VdsA2. Antimicrobial assays were performed by spot plate testing 100 μL of filter sterilized 10 μM VdsA1-P1A, VdsA2-P2A, and VdsA2-P2A or combinations thereof. The spot plates were performed on solid media (1% w/v agar) and added to the relevant growth medium seeded with each test strain, respectively.

Staphylococcus aureus subsp. *aureus* ATCC 25923, *S. aureus* subsp. *aureus* E2125, *P. aeruginosa* PAO1, *P. aeruginosa* ATCC 27853, *K. pneumoniae* K6 (ATCC 700603), *E. cloacae* ATCC 13047, *E. coli* ATCC 25299, and *B. subtilis* were cultured with Brain Heart Infusion (BHI) at 37 °C.*Vibrio harveyi*, *V. ruber*, and*T. viridans* XOM25T were cultured in Difco Marine Broth 2216, at 26 °C.*Saccharomyces cerevisiae* S288C,*C. neoformans* H99, and *C. albicans* CAB 1084 were cultured in yeast extract, peptone, dextrose (YPD).*Saccharomyces cerevisiae* S288C and *C. neoformans* H99 were grown at 30 °C, while*C. albicans* CAB 1084 was cultured at 37 °C.

Zebrafish Light−Dark Transition Assay. Ethical clearance for the zebrafish experiments was granted by the Stellenbosch University Research Ethics Committee: Animal Care and Use (reference no. ACU-2019-11820). Wild-type zebrafish eggs were obtained within 1 h of spawning in the zebrafish Research Unit in the Department of Medicine (Faculty of Medicine and Health Sciences, Stellenbosch University). Eggs and larvae were maintained in standard E3 embryo medium at 28 °C, with a 14/10 h light/dark cycle, and refreshed daily according to standard husbandry protocols.

The effects of VdsA1-P1A, VdsA2-P2A, and VdsA2-P2B alone, or in combination, on the behavioral responsiveness of zebrafish larvae (aged 118 h postfertilization) were assessed using the LDTT. Briefly, this entails pipetting individual larvae into wells on a 96-well plate and placing them into an automated activity tracker (DanioVision, Noldus, Germany) with onboard analytical software (EthoVision, Noldus, Germany). Each assay was 40 min long and consisted of an initial 10 min dark period (under infrared light to allow for larval movement tracking), which allows the larvae to acclimatize to their new environment. After this, basal activity was assessed from 10 to 20 min in darkness, before 10 min exposure to bright white light, which is known to trigger anxiety-like behavior (hyperlocomotion) in larvae as soon as the light is removed. The hyperlocomotion was assessed during a final 10 min dark period.

Zebrafish were exposed to peptides by immersion. VdsA1-P1A and VdsA2-P2A were tested at final concentrations of 0 (control), 2.5, 5.0, 10.0, and 20.0 μM, while VdsA2-P2B was only tested at 0, 2.5, 5.0, and 10.0 μM due to limited supply. TVdsA1-P1A and Vds-P2A were tested in combination, with final concentrations of 10.0 and 5.0 μM, respectively, as well as 10.0 and 10.0 μM, respectively. VdsA1-P1A and Vds-P2B were only tested in the combination of 10.0 and 5.0 μM, respectively. Behavioral tracking was performed after 1 and 24 h of continuous exposure to the peptides. At the end of the protocol, all larvae were killed by MS-222 overdose and subsequent freezing.

Statistical Procedure. The effect of VdsA1-P1A, VdsA2-P2A, VdsA2-P2B, and combinations thereof on zebrafish behavior was assessed by comparison to untreated controls. The effects of various peptide treatments at a range of concentrations was measured after 1 and 24 h of exposure by comparing the total locomotion over 10−20 min (basal activity state preillumination) and 30−40 min (excited state postillumination). At least n = 16 and a maximum of n = 41 zebrafish larvae per treatment group were used for statistical analysis.

Descriptive statistics are reported for each treatment's effect on zebrafish behavior. Each response variable was then analyzed with a one-way ANOVA. The normality of the residuals of the ANOVA was assessed with a normal probability plot, and the homogeneity of the group variances was tested with Levene's test. Nonparametric Kruskal−Wallis ANOVA was also performed if the residuals of the one-way ANOVA were not normally distributed. Fisher's LSD post hoc tests were used if the group variance was indeed homogeneous. If the Levene test indicates heteroscedasticity with a p-value less than 0.01, then Welch's ANOVA test was applied. The Games-Howell ad hoc test was then used for multiple comparisons of the group means. Due to the sedative effect, some data sets contained multiple 0 distance values, which caused heteroscedasticity and the Welch test to fail, but still called for application of the Games-Howell post hoc test.

For all analyses, the limit of statistical significance was set to $p < 0.05$. 95% confidence intervals (95% Cl) and are reported in the Supporting Information where appropriate. Analyses were done with Statistica 14 (TIBCO Software Inc. (2020), Data Science Workbench, version 14. http://TIBCO.com), SAS Enterprise Guide 7.1, and R 3.3.2.

CONCLUSIONS

Thalassomonas viridans XOM25T was isolated from a European flat oyster, *Ostrea edulis*, cultivated off the Mediterranean coast near Valencia. These oysters play a key role in the marine environment where they provide water quality and reef-building services to an undoubted wealth of species including many fish. The exact relationship between *O. edulis* and *T. viridans* XOM25T is yet to be described; however, the viridisin lanthipeptides could well be facilitating interactions between *O. edulis* and other higher organisms like fish. The biological role that neurologically active or interacting lanthipeptides may fulfill is largely unexplored but equally useful to society. Such findings contextualize the complexities of the natural world and make it difficult to avoid speculating about the exciting roles lanthipeptides can play. However, much work must still be

https://doi.org/10.1021/acsomega.4c03149
ACS Omega 2024, 9, 31832−31841

done with the viridisins and other lanthipeptides from Gram-negative bacteria to better define their biological activities and the exact modes and mechanisms behind their action.

■ ASSOCIATED CONTENT

Supporting Information

The Supporting Information is available free of charge at https://pubs.acs.org/doi/10.1021/acsomega.4c03149.

Experimental methods, HPLC-PR chromatograms, and all statistical procedure outputs (PDF)

■ AUTHOR INFORMATION

Corresponding Author

Ross Rayne Vermeulen − *Department of Microbiology, Stellenbosch University, Matieland 7602, South Africa; Institute for Microbial Biotechnology and Metagenomics, University of the Western Cape, Bellville 7535, South Africa;* orcid.org/0000-0002-2223-4364; Email: 16968018@sun.ac.za

Authors

Anton Du Preez van Staden − *Experimental Research Group, Faculty of Medicine and Health Sciences, Department of Medicine, Stellenbosch University, Parow 7499, South Africa;* orcid.org/0000-0003-0596-8849

Tracey Ollewagen − *Experimental Research Group, Faculty of Medicine and Health Sciences, Department of Medicine, Stellenbosch University, Parow 7499, South Africa*

Leonardo Joaquim van Zyl − *Institute for Microbial Biotechnology and Metagenomics, University of the Western Cape, Bellville 7535, South Africa*

Youran Luo − *Department of Chemistry and Howard Hughes Medical Institute, University of Illinois at Urbana−Champaign, Urbana, Illinois 61801, United States;* orcid.org/0000-0002-8033-2472

Wilfred A. van der Donk − *Department of Chemistry and Howard Hughes Medical Institute, University of Illinois at Urbana−Champaign, Urbana, Illinois 61801, United States;* orcid.org/0000-0002-5467-7071

Leon Milner Theodore Dicks − *Department of Microbiology, Stellenbosch University, Matieland 7602, South Africa;* orcid.org/0000-0002-5157-9046

Carine Smith − *Experimental Research Group, Faculty of Medicine and Health Sciences, Department of Medicine, Stellenbosch University, Parow 7499, South Africa;* orcid.org/0000-0001-5924-9204

Marla Trindade − *Institute for Microbial Biotechnology and Metagenomics, University of the Western Cape, Bellville 7535, South Africa;* orcid.org/0000-0002-2478-0270

Complete contact information is available at: https://pubs.acs.org/10.1021/acsomega.4c03149

Author Contributions

M.T, L.J.v.Z., and L.M.T.D initiated the study. A.D.P.vS and R.R.V designed the experimental procedure. R.R.V performed the cloning, lanthipeptide production, purification quantification, and antimicrobial screening. Y.L. performed stereochemical analysis. W.A.v.d.D and Y.L performed stereochemical data interpretation. C.S. and T.O. designed and performed the zebrafish screening assays. All authors participated in the data analysis, interpretation, and manuscript preparation.

Funding

This research was funded by the South African Medical Research Council (Self-Initiated grant), the DSI/NRF SARChI research chair in Microbial Genomics (UID87326), and the European Union under the Horizon Europe Program, Grant Agreement No. 101082304 (BlueRemediomics). Views and opinions expressed are however those of the author(s) only and do not necessarily reflect those of the European Union or the European Research Executive Agency (REA). Neither the European Union nor the granting authority can be held responsible for them.

Notes

The authors declare no competing financial interest.

■ ACKNOWLEDGMENTS

The authors would like to acknowledge the contribution of Prof Marina Rautenbach for her critical insights and advice. The authors would also like to thank Ray Sarksian for facilitating the stereochemical analysis. Finally, the authors would like to acknowledge and thank Dr. Mae Newton-Foot and the NHLS Microbiology Laboratory at Tygerberg Hospital for providing the strains used in this study, as well as Prof Jean Millar and Prof Robert Fenn for the financial support.

■ REFERENCES

(1) Thetsana, C.; Ijichi, S.; Kaweewan, I.; Nakagawa, H.; Kodani, S. Heterologous expression of a cryptic gene cluster from a marine proteobacterium Thalassomonas actiniarum affords new lanthipeptides thalassomonasins A and B. *J. Appl. Microbiol.* **2022**, *132*, 3629−3639.

(2) Han, Y.; Wang, X.; Zhang, Y.; Huo, L. Discovery and Characterization of marinsedin, a New Class II Lanthipeptide Derived from Marine Bacterium Marinicella sediminis F2T. *ACS Chem. Biol.* **2022**, *17*, 785−790.

(3) Smith, T. E.; et al. Accessing chemical diversity from the uncultivated symbionts of small marine animals. *Nat. Chem. Biol.* **2018**, *14*, 179−185.

(4) Caetano, T.; van der Donk, W.; Mendo, S. Bacteroidetes can be a rich source of novel lanthipeptides: The case study of Pedobacter lusitanus. *Microbiol Res.* **2020**, *235*, No. 126441.

(5) Wang, X.; et al. Deciphering the Biosynthesis of Novel Class I Lanthipeptides from Marine Pseudoalteromonas Reveals a dehydratase PsfB with Dethiolation Activity. *ACS Chem. Biol.* **2023**, *18*, 1218−1227.

(6) Arnison, P. G.; et al. ribosomally synthesized and post-translationally modified peptide natural products: overview and recommendations for a universal nomenclature. *Nat. Prod. Rep.* **2013**, *30*, 108−160.

(7) Repka, L. M.; Chekan, J. R.; Nair, S. K.; van der Donk, W. A. Mechanistic Understanding of Lanthipeptide Biosynthetic Enzymes. *Chem. Rev.* **2017**, *117*, 5457−5520.

(8) Knerr, P. J.; van der Donk, W. A. Chemical Synthesis of the Lantibiotic Lacticin 481 Reveals the Importance of lanthionine Stereochemistry. *J. Am. Chem. Soc.* **2013**, *135*, 7094−7097.

(9) Mukherjee, S.; Huo, L.; Thibodeaux, G. N.; van der Donk, W. A. Synthesis and Bioactivity of Diastereomers of the Virulence Lanthipeptide Cytolysin. *Org. Lett.* **2016**, *18*, 6188−6191.

(10) Hsu, S.-T. D.; et al. The nisin−lipid II complex reveals a pyrophosphate cage that provides a blueprint for novel antibiotics. *Nat. Struct Mol. Biol.* **2004**, *11*, 963−967.

(11) Sarksian, R.; van der Donk, W. A. Divergent Evolution of Lanthipeptide Stereochemistry. *ACS Chem. Biol.* **2022**, *17*, 2551−2558.

(12) Tang, W.; Jiménez-Osés, G.; Houk, K. N.; Van Der Donk, W. A. Substrate control in stereoselective lanthionine biosynthesis. *Nat. Chem.* **2015**, *7*, 57−64.

(13) Sarksian, R.; Hegemann, J. D.; Simon, M. A.; Acedo, J. Z.; van der Donk, W. A. Unexpected Methyllanthionine Stereochemistry in the Morphogenetic Lanthipeptide SapT. *J. Am. Chem. Soc.* **2022**, *144*, 6373−6382.
(14) van Staden, A. D. P.; van Zyl, W. F.; Trindade, M.; Dicks, L. M. T.; Smith, C. Therapeutic Application of Lantibiotics and Other Lanthipeptides: Old and New Findings. *Appl. Environ. Microbiol.* **2021**, *87*, No. e0018621.
(15) Begde, D.; et al. Immunomodulatory efficacy of nisin-a bacterial lantibiotic peptide. *Journal of Peptide Science* **2011**, *17*, 438−444.
(16) Shin, J. M.; et al. Biomedical applications of nisin. *J. Appl. Microbiol.* **2016**, *120*, 1449−1465.
(17) Barbosa, A. A. T.; de Melo, M. R.; da Silva, C. M. R.; Jain, S.; Dolabella, S. S. nisin resistance in Gram-positive bacteria and approaches to circumvent resistance for successful therapeutic use. *Crit Rev. Microbiol* **2021**, *47*, 376−385.
(18) Willey, J. M.; Willems, A.; Kodani, S.; Nodwell, J. R. Morphogenetic surfactants and their role in the formation of aerial hyphae in Streptomyces coelicolor. *Mol. Microbiol.* **2006**, *59*, 731−742.
(19) Kodani, S.; et al. The SapB morphogen is a lantibiotic-like peptide derived from the product of the developmental gene ramS in Streptomyces coelicolor. *Proc. Natl. Acad. Sci. U. S. A.* **2004**, *101*, 11448−53.
(20) Férir, G.; et al. The lantibiotic peptide labyrinthopeptin A1 demonstrates broad anti-HIV and anti-HSV activity with potential for microbicidal applications. *PLoS One* **2013**, *8*, No. e64010.
(21) Mohr, K. I.; et al. Pinensins: The First Antifungal Lantibiotics. *Angew. Chem., Int. Ed.* **2015**, *54*, 11254−11258.
(22) Lee, H.; Wu, C.; Desormeaux, E. K.; Sarksian, R.; van der Donk, W. A. Improved production of class I lanthipeptides in Escherichia coli. *Chem. Sci.* **2023**, *14*, 2537−2546.
(23) Bothwell, I. R.; Caetano, T.; Sarksian, R.; Mendo, S.; van der Donk, W. A. Structural Analysis of Class I Lanthipeptides from Pedobacter lusitanus NL19 Reveals an Unusual Ring Pattern. *ACS Chem. Biol.* **2021**, *16*, 1019−1029.
(24) Olonade, I.; van Zyl, L. J.; Trindade, M. Draft Genome Sequences of Marine Isolates of Thalassomonas viridans and Thalassomonas actiniarum. *Genome Announce.* **2015**, *3*, 7.
(25) Ivanova, E. P.; et al. Pseudoalteromonas maricaloris sp. nov., isolated from an Australian sponge, and reclassification of [Pseudoalteromonas aurantia] NCIMB 2033 as Pseudoalteromonas flavipulchra sp. nov. *Int. J. Syst. Evol Microbiol* **2002**, *52*, 263−271.
(26) Matu, A.; et al. Draft Genome Sequences of Seven Chryseobacterium Type Strains. *Microbiol Resour. Announce.* **2019**, *8*, 10.
(27) Gauthier, M. J. Alteromonas citrea, a New Gram-Negative, Yellow-Pigmented Species from Seawater. *Int. J. Syst. Bacteriol* **1977**, *27*, 349−354.
(28) Wang, X.-Q.; Li, C.-M.; Dunlap, C. A.; Rooney, A. P.; Du, Z.-J. Marinicella sediminis sp. nov., isolated from marine sediment. *Int. J. Syst. Evol Microbiol* **2018**, *68*, 2335−2339.
(29) Vermeulen, R.; Van Staden, A. D. P.; van Zyl, L. J.; Dicks, L. M. T.; Trindade, M. Unusual Class I Lanthipeptides from the Marine Bacteria Thalassomonas viridans. *ACS Synth. Biol.* **2022**, *11*, 3608−3616.
(30) Swinney, D. C.; Anthony, J. How were new medicines discovered? *Nat. Rev. Drug Discov* **2011**, *10*, 507−519.
(31) Zheng, W.; Thorne, N.; McKew, J. C. Phenotypic screens as a renewed approach for drug discovery. *Drug Discov Today* **2013**, *18*, 1067−73.
(32) Kiriiri, G. K.; Njogu, P. M.; Mwangi, A. N. Exploring different approaches to improve the success of drug discovery and development projects: a review. *Futur J. Pharm. Sci.* **2020**, *6*, 27.
(33) Croston, G. E. The utility of target-based discovery. *Expert Opin Drug Discov* **2017**, *12*, 427−429.
(34) Wiley, D. S.; Redfield, S. E.; Zon, L. I.; Wiley, D. S.; Redfield, S. E.; Zon, L. I. Chemical screening in zebrafish for novel biological and therapeutic discovery. *Methods in Cell Biology*; Academic Press Inc., 2017 Vol. *138*, 651−679.
(35) MacRae, C. A.; Peterson, R. T. zebrafish as tools for drug discovery. *Nat. Rev. Drug Discov* **2015**, *14*, 721−31.
(36) BLAST: Basic Local Alignment Search Tool. https://blast.ncbi.nlm.nih.gov/Blast.cgi. NIH. National Library of Medicine; National Center for Biotechnology Information.
(37) Pophaly, S. D.; Singh, R.; Pophaly, S. D.; Kaushik, J. K.; Tomar, S. K. Current status and emerging role of glutathione in food grade lactic acid bacteria. *Microbial. Cell Factories* **2012**, *11*, 114.
(38) Fahey, R. C.; Brown, W. C.; Adams, W. B.; Worsham', M. B. Occurrence of Glutathione in Bacteria. *J. Bacteriol.* **1978**, 1126.
(39) Powrie, Y.; et al. zebrafish behavioral response to ivermectin: insights into potential neurological risk. *Med. Drug Discov* **2022**, *16*, No. 100141.
(40) Sambrook, J.; Fritsch, E. F.; Maniatis, T. *Molecular cloning: a laboratory manual.*; Cold spring harbor laboratory press, 1989
(41) Ausubel, F. M.et al.Current protocols in molecular biology, edited by M. Ausubel, R. Brent; Kingston, R.E.; Moore, D.D.; Seidman, J.G.; Smith, J.A.; Struhl, K. Vol.s 1 and 2. John Wiley & Sons, Inc.: Media, PA, 1988, $165.00. Mol. Reprod. Dev. (1989) *1*, 146−146.
(42) Luo, Y.; Xu, S.; Frerk, A. M.; van der Donk, W. A. Facile Method for Determining Lanthipeptide Stereochemistry. *Anal. Chem.* **2024**, *96*, 1767.

https://doi.org/10.1021/acsomega.4c03149
ACS Omega 2024, 9, 31832−31841